Novel Growth Regime of MDCK II Model Tissues on Soft Substrates

Sara Kaliman,[†] Christina Jayachandran,[‡] Florian Rehfeldt,[‡*] and Ana-Sunčana Smith[†*]
[†]Institute for Theoretical Physics and Cluster of Excellence: Engineering of Advanced Materials, University Erlangen-Nürnberg, Germany; and [‡]3rd Institute of Physics - Biophysics, Georg-August-University, Göttingen, Germany

ABSTRACT It is well established that MDCK II cells grow in circular colonies that densify until contact inhibition takes place. Here, we show that this behavior is only typical for colonies developing on hard substrates and report a new growth phase of MDCK II cells on soft gels. At the onset, the new phase is characterized by small, three-dimensional droplets of cells attached to the substrate. When the contact area between the agglomerate and the substrate becomes sufficiently large, a very dense monolayer nucleates in the center of the colony. This monolayer, surrounded by a belt of three-dimensionally packed cells, has a well-defined structure, independent of time and cluster size, as well as a density that is twice the steady-state density found on hard substrates. To release stress in such dense packing, extrusions of viable cells take place several days after seeding. The extruded cells create second-generation clusters, as evidenced by an archipelago of aggregates found in a vicinity of mother colonies, which points to a mechanically regulated migratory behavior.

Received for publication 31 July 2013 and in final form 11 December 2013.

*Correspondence: rehfeldt@physik3.gwdg.de or smith@physik.fau.de

Studying the growth of cell colonies is an important step in the understanding of processes involving coordinated cell behavior such as tissue development, wound healing, and cancer progression. Apart from extremely challenging in vivo studies, artificial tissue models are proven to be very useful in determining the main physical factors that affect the cooperativity of cells, simply because the conditions of growth can be very well controlled. One of the most established cell types in this field of research is the Madin-Darby canine kidney epithelial cell (MDCK), originating from the kidney distal tube (1). A great advantage of this polarized epithelial cell line is that it retained the ability for contact inhibition (2), which makes it a perfect model system for studies of epithelial morphogenesis.

Organization of MDCK cells in colonies have been studied in a number of circumstances. For example, it was shown that in three-dimensional soft Matrigel, MDCK cells form a spherical enclosure of a lumen that is enfolded by one layer of polarized cells with an apical membrane exposed to the lumen side (3). These structures can be altered by introducing the hepatocyte growth factor, which induces the formation of linear tubes (4). However, the best-studied regime of growth is performed on two-dimensional surfaces where MDCK II cells form sheets and exhibit contact inhibition. Consequently, the obtained monolayers are well characterized in context of development (5), mechanical properties (6), and obstructed cell migration (7–9).

Surprisingly, in the context of mechanics, several studies of monolayer formation showed that different rigidities of polydimethylsiloxane gels (5) and polyacrylamide (PA) gels (9) do not influence the nature of monolayer formation nor the attainable steady-state density. This is supposedly due to long-range forces between cells transmitted by the underlying elastic substrate (9). These results were found to agree well with earlier works on bovine aortic endothelial cells (10) and vascular smooth muscle cells (11), both reporting a lack of sensitivity of monolayers to substrate elasticity. Yet, these results are in stark contrast with single-cell experiments (12–15) that show a clear response of cell morphology, focal adhesions, and cytoskeleton organization to substrate elasticity. Furthermore, sensitivity to the presence of growth factors that are dependent on the elasticity of the substrate in two (16) and three dimensions (4) makes this result even more astonishing. Therefore, we readdress the issue of sensitivity of tissues to the elasticity of the underlying substrate and show that sufficiently soft gels induce a clearly different tissue organization.

We plated MDCK II cells on soft PA gels (Young's modulus $E = 0.6 \pm 0.2$ kPa), harder PA gels ($E = 5$, 11, 20, 34 kPa), and glass, all coated with Collagen-I. Gels were prepared following the procedure described in Rehfeldt et al. (17); rigidity and homogeneity of the gels was confirmed by bulk and microrheology (see the Supporting Material for comparison). Seeding of MDCK II cells involved a highly concentrated solution dropped in the middle of a hydrated gel or glass sample. For single-cell

Editor: Paul Wiseman.

http://dx.doi.org/10.1016/j.bpj.2013.12.056

experiments, cells were dispersed over the entire dish. Samples were periodically fixed up to Day 12, stained for nuclei and actin, and imaged with an epifluorescence microscope. Details are described in the Supporting Material.

On hard substrates and glass it was found previously that the area of small clusters expands exponentially until the movement of the edge cannot keep up with the proliferation in the bulk (5). Consequently, the bulk density increases toward the steady state, whereas the density of the edge remains low. At the same time, the colony size grows subexponentially (5). This is what we denote "the classical regime of growth". Our experiments support these observations for substrates with $E \geq 5$ kPa. Specifically, on glass, colonies start as small clusters of very low density of 700 ± 200 cells/mm^2 (Fig. 1, *A* and *B*), typically surrounded by a strong actin cable (Fig. 1, *B* and *C*). Interestingly, the spreading area of single cells (Fig. 1 *A*) on glass was found to be significantly larger, i.e., $(2.0 \pm 0.9) \times 10^{-3}$ mm^2. After Day 4 (corresponding cluster area of 600 ± 100 mm^2), the density in the center of the colony reached the steady state with $6{,}800 \pm 500$ cells/mm^2, whereas the mean density of the edge profile grew to $4{,}000 \pm 500$ cells/mm^2. This density was retained until Day 12 (cluster area 1800 ± 100 mm^2), which is in agreement with previous work (9).

In colonies grown on 0.6 kPa gels, however, we encounter a very different growth scenario. The average spreading area of single cells is $(0.34 \pm 0.3) \times 10^{-3}$ mm^2, which is six times smaller than on glass substrates (Fig. 2 *A*). Clusters of only few cells show that cells have a preference for cell-cell contacts (a well-established flat contact zone can be seen at the cell-cell interface in Fig. 2 *A*) rather than for cell-substrate contacts (contact zone is diffusive and the shape of the cells appears curved). The same conclusion

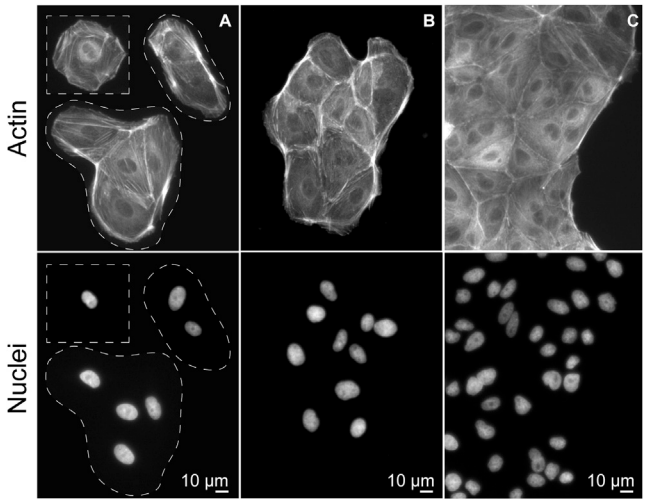

FIGURE 1 Early phase of cluster growth on hard substrates. (*A*) Well-spread single cells, and small clusters with a visible actin cable 6 h after seeding. (*B*) Within one day, clusters densify and merge, making small colonies. (*C*) Edge of clusters from panel *B*.

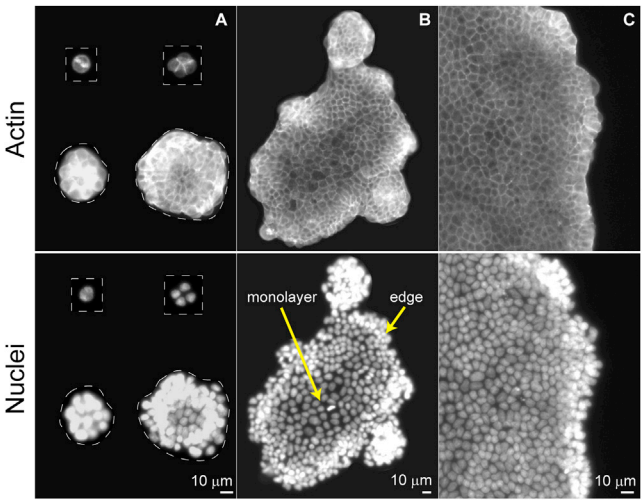

FIGURE 2 Early phase of cluster growth on soft substrates. (*A*) Twelve hours after seeding, single cells remain mostly round and small. They are found as individual, or within small, three-dimensional structures (*top*). The latter nucleate a monolayer in their center (*bottom*), if the contact area with the substrate exceeds ~5×10^{-3} mm^2. (*B*) Irregularly-shaped clusters appear due to merging of smaller droplets. A stable monolayer surrounded by a three-dimensional belt of densely packed cells is clearly visible, even in larger structures. (*C*) All colonies are recorded on Day 4.

emerges from the fact that dropletlike agglomerates, resting on the substrate, form spontaneously (Fig. 2 *A*), and that attempts to seed one single cluster of 90,000 cells fail, resulting in a number of three-dimensional colonies (Fig. 2 *A*). When the contact area with the substrate exceeds 4.7×10^{-3} mm^2, a monolayer appears in the center of such colonies (Fig. 2 *B*). The colonies can merge, and if individual colonies are small, the collapse into a single domain is associated with the formation of transient irregular structures (Fig. 2 *B*). Ultimately, large elliptical colonies (average major/minor axis of $e = 1.8 \pm 0.6$) with a smooth edge are formed (Fig. 2 *C*), unlike on hard substrates where circular clusters ($e = 1.06 \pm 0.06$) with a ragged edge comprise the characteristic phenotype.

Irrespective of cluster size, in the new regime of growth, the internal structure is built of two compartments (Fig. 2 *B*):

1. The first is the edge (0.019 ± 0.05-mm wide), a three-dimensional structure of densely packed cells. This belt is a signature of the new regime because on hard substrates the edge is strictly two-dimensional (Fig. 1 *C*).
2. The other is the centrally placed monolayer with a spatially constant density that is very weakly dependent on cluster size and age (Fig. 3). The mean monolayer density is $13{,}000 \pm 2{,}000$ cells/mm^2, which is an average over 130 clusters that are up to 12 days old and have a size in the range of 10^{-3} to 10 mm^2, each shown by a data point in Fig. 3. This density is twice the steady-state density of the bulk tissue in the classical regime of growth.

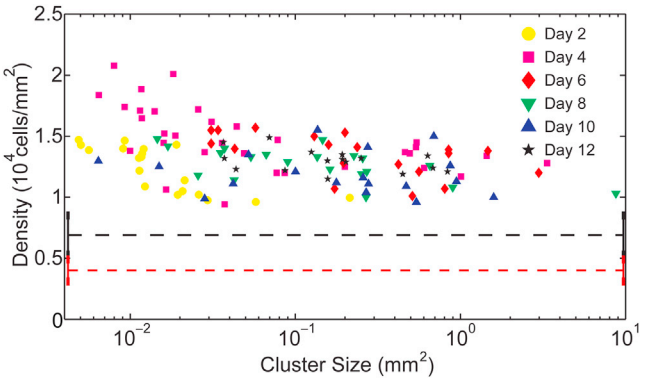

FIGURE 3 Monolayer densities in colonies grown on 0.6 kPa substrates, as a function of the cluster size and age. Each cluster is represented by a single data point signifying its mean monolayer density. (*Black lines*) Bulk and (*red dashed lines*) edge of steady-state densities from monolayers grown on glass substrates. Error bars are omitted for clarity, but are discussed in the Supporting Material.

Until Day 4, the monolayer is very homogeneous, showing a nearly hexagonal arrangement of cells. From Day 4, however, defects start to appear in the form of small holes (typical size of $(0.3 \pm 0.1) \times 10^{-3}$ mm^2). These could be attributed to the extrusions of viable cells, from either the belt or areas of increased local density in the monolayer (*inset* in Fig. 4). This suggests that extrusions serve to release stress built in the tissue, and, as a consequence, the overall density is decreased.

Previous reports suggest that isolated MDCK cells undergo anoikis 8 h after losing contact with their neighbors (18). However, in this case, it appears that instead of dying, the extruded cells create new colonies, which can be seen as an archipelago surrounding the mother cluster (Fig. 4). The viability of off-cast cells is further evidenced by the appearance of single cells and second-generation colonies with sizes varying over five orders of magnitude, from Day 4 until the end of the experiment, Day 12. Importantly, no morphological differences were found in the first- and second-generation colonies.

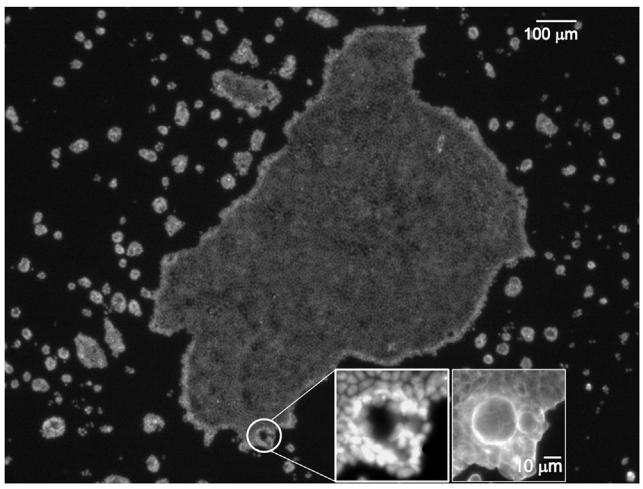

FIGURE 4 Cell nuclei within the mother colony and in the neighboring archipelago of second-generation clusters grown on 0.6 kPa gels at Day 12. (*Inset*; *scale bar* = 10 μm) Scar in the tissue, a result of a cell-extrusion event. (*Main image*; *scale bar* = 100 μm) From the image of cell nuclei (*left*), it is clear that there are no cells within the scar, whereas the image of actin (*right*) shows that the cytoplasm of the cells at the edge has closed the hole.

In conclusion, we show what we believe to be a novel phase of growth of MDCK model tissue on soft PA gels ($E = 0.6$ kPa) that, to our knowledge, despite previous similar efforts (9), has not been observed before. This finding is especially interesting in the context of elasticity of real kidneys, for which a Young's modulus has been found to be between 0.05 and 5 kPa (19,20). This coincides with the elasticity of substrates studied herein, and opens the possibility that the newly found phase of growth has a particular biological relevance. Likewise, the ability to extrude viable cells may point to a new migratory pathway regulated mechanically by the stresses in the tissue, the implication of which we hope to investigate in the future.

SUPPORTING MATERIAL

Materials and Methods (including one equation), Data Analysis (with subsections Single Cells, Glass and Hard Substrates, and Soft Substrates), two figures, and References (21,22) are available at http://www.biophysj.org/biophysj/supplemental/S0006-3495(14)00220-3.

ACKNOWLEDGMENTS

This work was in part (F.R.) funded by the Deutsche Forschungsgemeinschaft (DFG) within the SFB 755-B8. A.-S. S. and S. K. acknowledge funding from European Research Council Starting Grant MembranesAct No. 337283.

REFERENCES and FOOTNOTES

1. Herzlinger, D. A., T. G. Easton, and G. K. Ojakian. 1982. The MDCK epithelial cell line expresses a cell surface antigen of the kidney distal tubule. *J. Cell Biol.* 93:269–277.
2. Rothen-Rutishauser, B., S. D. Krämer, …, H. Wunderli-Allenspach. 1998. MDCK cell cultures as an epithelial in vitro model: cytoskeleton and tight junctions as indicators for the definition of age-related stages by confocal microscopy. *Pharm. Res.* 15:964–971.
3. Wang, C. C., L. Jamal, and K. A. Janes. 2012. Normal morphogenesis of epithelial tissues and progression of epithelial tumors. *Wiley Interdiscip. Rev. Syst. Biol. Med.* 4:51–78.
4. Wells, E. K., O. Yarborough, 3rd, …, M. J. Caplan. 2013. Epithelial morphogenesis of MDCK cells in three-dimensional collagen culture is modulated by interleukin-8. *Am. J. Physiol. Cell Physiol.* 304:C966–C975.
5. Puliafito, A., L. Hufnagel, …, B. I. Shraiman. 2012. Collective and single cell behavior in epithelial contact inhibition. *Proc. Natl. Acad. Sci. USA.* 109:739–744.
6. Harris, A. R., L. Peter, …, G. T. Charras. 2012. Characterizing the mechanics of cultured cell monolayers. *Proc. Natl. Acad. Sci. USA.* 109:16449–16454.

7. Angelini, T. E., E. Hannezo, …, D. A. Weitz. 2010. Cell migration driven by cooperative substrate deformation patterns. *Phys. Rev. Lett.* 104:168104.
8. Angelini, T. E., E. Hannezo, …, D. A. Weitz. 2011. Glass-like dynamics of collective cell migration. *Proc. Natl. Acad. Sci. USA.* 108:4714–4719.
9. Trepat, X., M. R. Wasserman, …, J. J. Fredberg. 2009. Physical forces during collective cell migration. *Nat. Phys.* 5:426–430.
10. Yeung, T., P. C. Georges, …, P. A. Janmey. 2005. Effects of substrate stiffness on cell morphology, cytoskeletal structure, and adhesion. *Cell Motil. Cytoskeleton.* 60:24–34.
11. Sazonova, O. V., K. L. Lee, …, J. Y. Wong. 2011. Cell-cell interactions mediate the response of vascular smooth muscle cells to substrate stiffness. *Biophys. J.* 101:622–630.
12. Pelham, Jr., R. J., and Y. L. Wang. 1997. Cell locomotion and focal adhesions are regulated by substrate flexibility. *Proc. Natl. Acad. Sci. USA.* 94:13661–13665.
13. Discher, D. E., P. Janmey, and Y. L. Wang. 2005. Tissue cells feel and respond to the stiffness of their substrate. *Science.* 310:1139–1143.
14. Nemir, S., and J. L. West. 2010. Synthetic materials in the study of cell response to substrate rigidity. *Ann. Biomed. Eng.* 38:2–20.
15. Zemel, A., F. Rehfeldt, …, S. A. Safran. 2010. Cell shape, spreading symmetry and the polarization of stress-fibers in cells. *J. Phys. Condens. Matter.* 22:194110.
16. Leight, J. L., M. A. Wozniak, …, C. S. Chen. 2012. Matrix rigidity regulates a switch between TGF-β1-induced apoptosis and epithelial-mesenchymal transition. *Mol. Biol. Cell.* 23:781–791.
17. Rehfeldt, F., A. E. Brown, …, D. E. Discher. 2012. Hyaluronic acid matrices show matrix stiffness in 2D and 3D dictates cytoskeletal order and myosin-II phosphorylation within stem cells. *Integr. Biol. (Camb.).* 4:422–430.
18. Frisch, S. M., and H. Francis. 1994. Disruption of epithelial cell-matrix interactions induces apoptosis. *J. Cell Biol.* 124:619–626.
19. Levental, I., P. C. Georges, and P. A. Janmey. 2006. Soft biological materials and their impact on cell function. *Soft Matter.* 2:1–9.
20. Han, Y. 2009. The Role of Mechanical Forces in Regulation of Focal Adhesion Complex Proteins in Developing Kidney. Department of Physiology, National Cheng Kung University, Tainan, Taiwan.
21. Rasband, W. S. 1997–2012. IMAGEJ. U.S. National Institutes of Health, Bethesda, MD. *http://imagej.nih.gov/ij/.*
22. Otsu, N. 1979. A threshold selection method from gray-level histograms. *IEEE Trans.* 9:62–66.

Novel growth regime of MDCK II model tissues on soft substrates

Sara Kaliman,[1] Christina Jayachandran,[2] Florian Rehfeldt,[2] Ana-Sunčana Smith[1]

[1] Institute for Theoretical Physics and Cluster of Excellence: Engineering of Advanced Materials, University Erlangen-Nürnberg, Germany
[2] 3rd Institute of Physics - Biophysics, Georg-August-University, Göttingen, Germany

MATERIALS AND METHODS

MDCK II cells (#00062107) were obtained from ECACC (UK) and cultured in MEM with Earle´s Salts (# F0325, Biochrom) supplemented with 2mM L-glutamin (# G7513, Sigma-Aldrich), 5% FBS (#F0804, Sigma-Aldrich) and 1% Penn/Strep (#15070-063, Gibco, LifeTechnologies) at 37° C and 5 % CO_2. Cells were split and passaged every other day to keep them sub-confluent (< 80%).

Collagen-I (BD Biosciences) coated elastic polyacrylamide (PA) gels were prepared as described earlier [Ref 15 in the main text] adapted from the original protocol by Pelham and Wang [Ref 11 in the main text]. The Young's elastic modulus E was measured by macro rheology (MCR 501, Anton Paar, Austria) using a cone and plate geometry (Ø = 25 mm, 2°) A typical gelation curve of PA yielding a shear storage modulus G' = after 1h (3,600 s), the usual polymerization time for PA gels is shown in Fig S1A. This is converted to the Young's modulus E using a Poisson's ratio of $\nu = 0.45$ (Engler et al., Meth Cell Biol, 83 (2007) 521). To ensure a homogeneous elastic hydrogel, the macroscopic rheology measurements were complemented with microrheology using atomic force microscopy (AFM, MFP-3D, Asylum Research, Santa Barbara, USA). The resulting force-indentation curves were fitted using a modified Hertz model

$$E = \frac{\pi \left(1-\nu^2\right) F}{\delta^2 \; 2 \tan \alpha}$$

as described in (Engler et al., Meth Cell Biol, 83 (2007) 521) and shown in Fig S1B (black line depicts experimental data, dotted red line shows the fitted Hertz model).

To assure similar collagen-I coating, glass slides were cleaned and treated with the same cross-linker (Sulfo-SANPAH, Pierce, Thermo Scientific) before collagen incubation as described.

MDCK II cells were seeded in two different ways on substrates. First, 30,000 cells were dispersed over the whole area of the substrate to investigate single cell behaviour and the onset of cluster formation. Second, cells were seeded as a highly concentrated (90,000 cells in 7 µL) drop in the middle of the sample, subsequently incubated for one hour before gently adding 2 mL of medium.

Filamentous actin was stained using phalloidin–tetramethylrhodamine B isothiocyanate (#77418-100UG, Sigma-Aldrich) and the nucleus was labelled with Hoechst 33342 trihydrochloride trihydrate (Molecular Probes, Life Technologies). Fluorescence microscopy was performed on a Zeiss Cell Obsever Z1 using 5 x, 20 x and 32 x objectives and images were recorded with a Zeiss AxioCam M3 and the Zeiss AxioVision software package (all Zeiss, Göttingen).

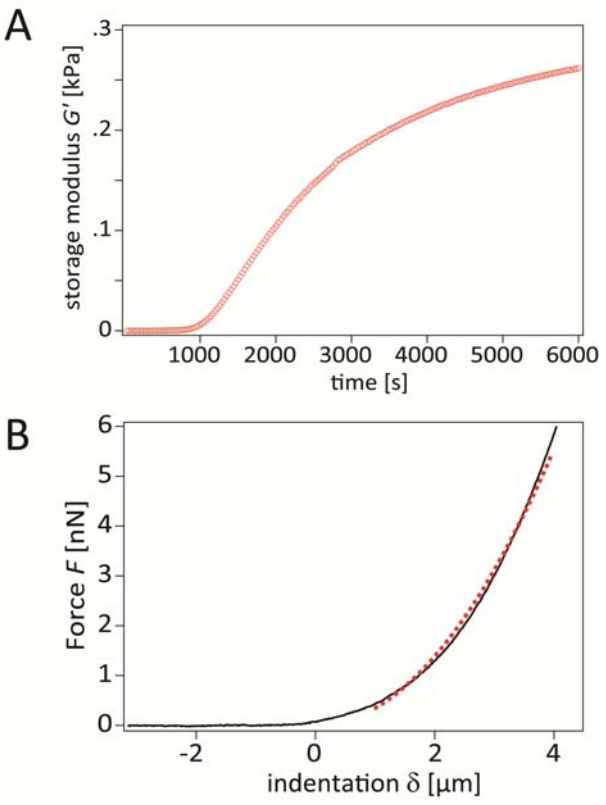

Fig. S1. *A*) A typical polymerization curve of PA yielding a shear storage modulus. *B*) Atomic force microscopy force-indentation curves. The black line depicts experimental data, dotted red line shows the fitted Hertz model.

DATA ANALYSIS

SINGLE CELLS

Single cell area was determined after segmentation of actin images as the area of white objects. Error in threshold procedure is negligible compared to variation of the cell size. There are 50 cells in statistics for glass substrate and 90 cells for 0.6 kPa PA gels.

GLASS AND HARD SUBSTRATES

Image analysis was performed with self-developed routines in MALAB (The MathWorks, Natick, MA, USA). The density of large colonies was obtained from an automated procedure whereby the number of objects in a given area was determined from segmented fluorescence images of cell nuclei (Fig SI2*A*). The reported values are spatial averages from the bulk and the edge parts of the cluster performed independently at a fixed instance of time (days 4-12). The averaging is performed over images of a colony on a given day (4, 6,...12) and then over all days.

The error in determination of density emerges when two nuclei are recognized as one (green ellipse in Fig. S2A), or when one nuclei is recognized as two (yellow ellipses in Fig. S2A). The relative error in cell density arising from this effects amounts to 2%, which is calculated after determining the density from images with corrected nuclei recognition step. Since this induces a small error, the reported standard deviation entirely reflects the fluctuations of the cell density within the respective colony compartments. Another reason for a large deviation is that the data set includes colonies of different age. On a level of a single colony at a particular day, the bulk density is at least fifty percent larger than the density in the edge of the cluster.

The area of a large colony is determined by approximating the shape of the cluster by an ellipse, and measuring the minor and major axis. The reported error corresponds to the standard deviation of cluster sizes from several experiments, which is again significantly larger than the error in determining the area of a single colony.

SOFT SUBSTRATES

The density and the monolayer area in small clusters was determined with ImageJ (Rasband, W.S., ImageJ, U. S. National Institutes of Health, Bethesda, Maryland, USA, http://imagej.nih.gov/ij/, 1997-2012). Thereby, the number of cell nuclei was counted within area of interest, the latter being determined with a freehand selection tool (Fig S2B). Deviation arising from repeatedly selecting the same area is less than 1%. The main contribution to the reported deviation comes from the variation in density when changing the area of interest. Examples of areas of interest are shown in different colours in Fig. S2B. Nevertheless, the relative uncertainly in density remains below 10%, and naturally becomes smaller as the size of the monolayer increases. For example, the area of the monolayer of the colony shown in Fig S2B is determined with the 6% relative uncertainty.

For bigger clusters the same procedure to determine the number of cells in a given image was used as for colonies on hard substrates. On the other hand, the size of the colony was determined after segmenting the images using the Otsu's method (for details see Otsu, N. 1979. A Threshold Selection Method from Gray-Level Histograms. *IEEE Transactions on Systems, Man, and Cybernetics*. 9:62-66). For very large colonies a collage of images was made prior to segmentation. In total, 130 colonies were analysed with sizes differing over five orders of magnitude.

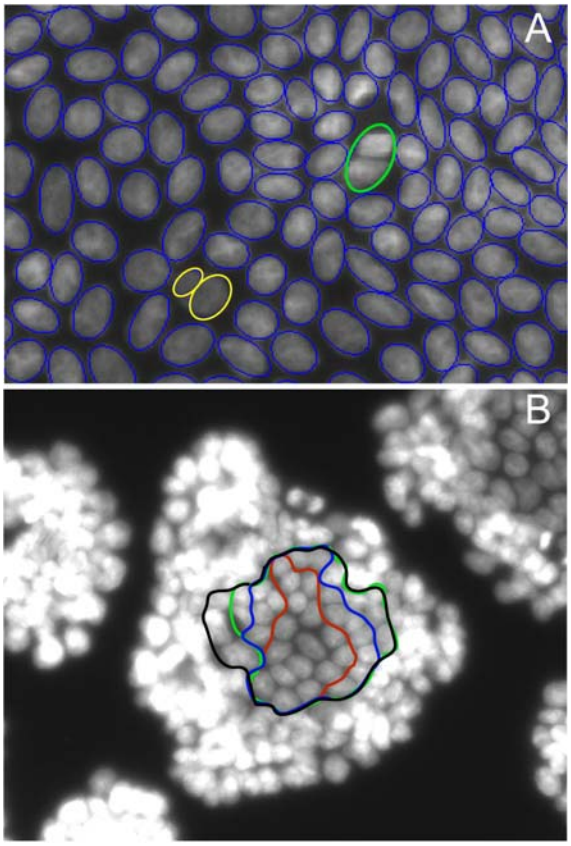

FIGURE S2 Sources of errors in determining the cell density. (A) The MATLAB routine may recognize two nuclei as one object (green) or divide one nucleus into two objects (yellow). This leads to total error of 2%. (B) Freehand selection tool in ImageJ and four possible monolayer areas of interest. The four selections lead to a 6% relative uncertainty in determining the cell density.